Journal of Natural Resources and Environmental Management
https://doi.org/10.29244/jpsl.14.2.325

RESEARCH ARTICLE

OPEN ACCESS

Check for updates

Comparisons of Growth, Yield, and Meteorological Properties of Rice Canopy under Double-Row (*Jajar Legowo* and *Jejer Manten*) and Tile Transplanting Systems

Taufiq Yuliawan[a,b], Nazif Ichwan[a,c], Augustine Ukpoju[a], Fadli Irsyad[d], Hiroki Oue[e]

[a] The United Graduate School of Agricultural Sciences, Ehime University, Matsuyama, Ehime, 790-8566, Japan
[b] Environmental Research Center, IPB University, Bogor, West Java, 16680, Indonesia
[c] Faculty of Agriculture, Universitas Sumatera Utara, Medan, North Sumatera, 20155, Indonesia
[d] Faculty of Agricultural Technology, Andalas University, Limau Manis, Padang, 25163, Indonesia
[e] Graduate School of Agriculture, Ehime University, Matsuyama, Ehime, 790-8566, Japan

Article History
Received 19 April 2024
Revised 22 May 2024
Accepted 01 June 2024

Keywords
border effect, double row, sink capacity, sink filling rate, NDVI

ABSTRACT

Over the past decade, the Indonesian government has been recommending double-row transplanting systems, i.e., *Jajar Legowo* (JL) and *Jejer Manten* (JM), to increase rice production. These systems have been reported to obtain higher yield of Indica rice cultivars than the standard tile (TL) system, primarily due to the border effect. However, scientific investigations of the border effect in these transplanting systems remain limited. This study was conducted during the summer seasons in Japan in 2022 and 2023 to observe the plant growth and yield of a Japonica rice cultivar, Nikomaru, and to investigate differences in meteorological properties, such as intercepted solar radiation (SR_{int}). The study found that higher plant competition for light in JM and JL caused a lower tiller number and above-ground biomass (W_t) per hill than in TL. However, due to denser planting, JM and JL obtained higher tiller numbers, W_t, and sink capacity per unit area than TL. Additionally, the denser canopy in JM and JL compared to TL increased SR_{int} by the whole canopy, even though the space between the double rows was wider. Although SR_{int} was not significantly different among the systems, higher normalized difference vegetation index in JM and JL was strongly correlated with a higher sink filling rate due to the healthier canopy absorbing more solar radiation. The synergistic effect of higher sink capacity and sink filling rate led to higher yields in JM and JL than in TL. This study suggests that JM is the best transplanting system for increasing rice yield.

Introduction

Rice is a staple food for most Asian countries, particularly Indonesia and Japan. Over the last five years, milled rice production in Indonesia and Japan has been lower than consumption levels [1]. The IPCC (Intergovernmental Panel on Climate Change) has reported that global warming could further reduce rice yields [2] by decreasing both the quantity (e.g., [3]) and quality (e.g., [4]) of rice. Therefore, sustainable rice production in Indonesia and Japan is a critical food security issue. In order to cope with these problems, the Indonesian government has implemented rice intensification strategies, including the adoption of transplanting systems designed to increase rice production. One such system is the double-row transplanting system, *Jajar Legowo* (JL), which has been shown to significantly increase yields compared to the standard tile transplanting system [5,6]. The JL transplanting system was introduced in 1994 [7] and adopted as a national agricultural program in 2013 [8]. The most recommended JL system is JL 2:1, with 12.5 cm, 25.0 cm, and 50.0 cm spacing between columns, between rows, and between double rows, respectively [6]. In addition to JL, some farmers practice a modified double-row transplanting system called *Jejer Manten* (JM), which involves pairing two plants with 5 cm spacing between the paired plants, 30 cm between columns, and 30 cm

Corresponding Author: Hiroki Oue oue.hiroki.mh@ehime-u.ac.jp Graduate School of Agriculture, Ehime University, Matsuyama, Ehime, Japan.

between double rows. A previous study [9] found that JM could achieve a 6% higher yield than JL 2:1. Both JM and JL are considered double-row transplanting systems because the space adjustments compact the plants into two rows, increasing the plant population while maintaining a large space between the double rows.

Previous studies have shown that the double-row transplanting system can increase the yield of Indica rice compared to the standard tile transplanting system (TL). For example, cultivar Sertani 14 [10] and IPB 3S [11] have shown increased yields with the JL system, while cultivar Inpari-10 [9,12] has shown increased yields with the JM system. In Japan, the double-row transplanting system is not commonly used; Japanese farmers typically use a tile transplanting system, for example, 30 cm wide and 16 cm long spacing between plants [13]. This study aimed to apply JM and JL to a Japonica rice cultivar, Nikomaru, with the expectation that these double-row transplanting systems would increase the yield of Nikomaru in Japan.

The normalized difference vegetation index (NDVI) is widely used for monitoring vegetation conditions, such as vegetation density (e.g., [14]). Kriegler et al. [15] introduced the NDVI as a vegetation index for quantifying the health and density of the canopy. NDVI is derived from the radiance of near-infrared and red spectrums. Healthy vegetation absorbs a lot of visible light and reflects and emits more near-infrared spectrum compared to unhealthy vegetation [16]. Thus, higher NDVI values indicate healthier vegetation, which can absorb more solar radiation for photosynthetic activity. Previous studies have reported a strong relationship between NDVI and absorbed solar radiation [17].

A higher yield in the double-row transplanting systems (i.e., JM and JL) compared to TL might be influenced by the border effect [9,18]. The border effect occurs when the plants on the outermost row or border of the rice field experience better environmental conditions, such as higher solar radiation and better air circulation [19], which can increase rice yield [19–21]. However, although previous research has compared the yields of JM and JL with TL and attributed the results to the border effect, the border effect in JM and JL is not fully understood and lacks sufficient information. This study addresses whether double-row transplanting systems can increase rice yield and alter the micrometeorological conditions within the rice canopy. Additionally, this study monitors NDVI to assess differences in healthy above-ground biomass in response to the change in the transplanting system.

Materials and Methods

Materials for The Experiment

Field experiments were conducted during the summer seasons of 2022 and 2023. In 2022, Nikomaru was sown on May 29 and transplanted on June 18, while in 2023, Nikomaru was sown on May 27 and transplanted on June 17. The sowing was conducted in wet-bed nurseries, and transplanting was manually done by transplanting three selected seedlings per hill. The seedlings were selected based on their height. The research plot was located on the experimental rice field at the Faculty of Agriculture, Ehime University, Matsuyama, Japan (33°50' N, 132°47' E), surrounded by experimental upland plantations (e.g., apples), screen houses, greenhouses, and workshops. Other researchers also transplanted various rice cultivars, mainly Hinohikari, in the same experimental rice field. The arrangement of the research plot was consistent in 2022 and 2023, but the size of the research plot was 95.0 m^2 in 2022 [22] and 171.0 m^2 in 2023. The layout of the research plot in 2023 is shown in Figure 1a.

Compound fertilizer was applied to the field as basal dressing with a 4:6:4 g m^{-2} ratio of N, P_2O_5, and K_2O. The water level in the field was continuously maintained at around 3–5 cm. Mid-season drainage was applied from July 15 to 25, 2022. The transplanting systems used in this study were TL, JM, and JL 2:1, with hill densities of 16.00, 19.05, and 21.33 hills m^{-2}, respectively. TL, JM, and JL have different row spacings of 25 cm, 5 cm, and 25 cm, respectively, and the spacings between the columns in each transplanting system are 25.0 cm, 30.0 cm, and 12.5 cm, respectively. The spacings between the double rows in JM and JL are 30 cm and 50 cm, respectively. The hill arrangement in each transplanting system is shown in Figure 1b.

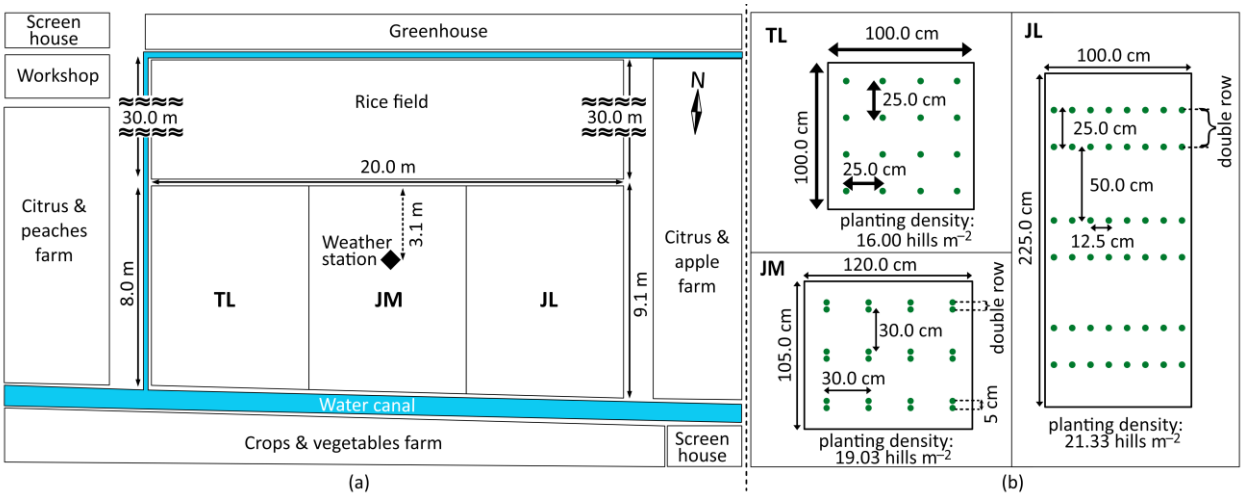

Figure 1. Illustration of (a) the research plot in 2023 and (b) the transplanting systems used in 2022 and 2023.

Measurement of Plant Growth Parameters, Yield, And Production

Plant growth parameters, such as tiller number and canopy height, were observed weekly from 10 hill samples. Three hill samples were selected based on the average condition of plant growth parameters for observing the leaf area index (LAI), which was calculated by leaf number and size (width, length, and leaf area ratios), as shown in Equation 1. The leaf area ratios were obtained by comparing the calculated leaf area with the leaf area from the destructive sample, measured by a leaf area meter (LI-3000, Licor, USA). The LAI calculated by the non-destructive method was adjusted to match the measured LAI of the destructive sample.

$$A_{leaf} = l_{leaf} \times w_{leaf} \times \alpha_{leaf} \quad (1)$$

where A_{leaf} (cm^2) is calculated leaf area, l_{leaf} (cm) is the leaf length, w_{leaf} (cm) is the leaf width, and α_{leaf} is the ratio of length and width to the leaf area. The α_{leaf} values were 0.62 (initial stage), 0.72 (initial–maximum tiller stage), and 0.71 (maximum tiller stage–harvest). The α_{leaf} values were derived from single-leaf areas measured with the LI-3000, and the length and width of single-leaf samples measured with a ruler.

The rice was harvested 110 days after transplanting in both years (October 6, 2022, and October 5, 2023). Above-ground biomass and yield were taken from three sampling areas in each transplanting system, with each sampling area consisting of three hill samples. The samples were selected based on the average plant growth condition of 10 hill samples. After being air-dried for ten days, the harvested samples (excluding spikelets) were oven-dried for 48 hours at 80 °C. Spikelets were treated separately to observe yield components.

The yield of brown rice was calculated from yield components such as total spikelet number per panicle, percentage of mature or filled grain, weight of 1,000 grains (brown rice), and grain moisture, as shown in Equation 2. Mature and immature grains were separated by soaking them in a water and salt solution with a density of 1.06 g m^{-3} (e.g., [23]). The number of grains was measured using a seed counter, Ooyatanzo DT-OT (Ohya Tanzo Factory, Japan). Brown rice was obtained by removing the husk with a mini rice huller machine, MH-D (Otake Manufacturer, Japan). Grain moisture was measured with a grain moisture meter, CD-6 (Shizuoka Seiki, Japan). Brown rice weight was adjusted to 15% of grain moisture (e.g., [24]). Sink capacity, the potential weight of spikelets or grain, is calculated from the total grain number and the weight of 1,000 grains [25], as displayed in Equation 3. The sink filling rate was assumed to be the same as the percentage of filled grain. To compare the averages of plant growth parameters, above-ground biomass, yield, and yield components between the transplanting systems, a paired t-test at a 5% significance level, corrected with the Bonferroni test (n=3), was used.

$$\text{Yield} = \frac{\text{number of hills}}{\text{m}^2} \times \frac{\text{number of panicles}}{\text{hill}} \times \frac{\text{number of grains}}{\text{panicle}} \times \frac{W_{1,000g}}{1,000} \times \text{filled grains} \quad (2)$$

$$\text{Sink capacity} = \text{number of grains} \times \frac{W_{1,000g}}{1,000} \quad (3)$$

where yield (g m^{-2}) is the yield of brown rice at 15% of grain moisture, $W_{1,000g}$ (g) is the weight of 1,000 grains of brown rice at 15% grain moisture, filled grains (%) is the percentage of filled or mature grains, and sink capacity (g m^{-2}) is the potential weight of grain.

Measurements and Analysis of Meteorological Properties

Solar radiation above the canopy (*SR*) was measured using a net radiometer CNR4 (Kipp & Zonen, Netherlands) at the height of 1.2 m (initial–flag leaf extension) and 1.5 m (flag leaf extension–harvesting). Air temperature (T_a) and relative humidity (RH) at a height of 2.0 m were measured using a temperature and humidity probe HMP155 (Vaisala, Finland) with a ventilated system PVC-04 (Prede, Japan). Photosynthetically active radiation (PAR) above the canopy (PAR_a) at the same height as the CNR4 was measured using a spot-type PAR sensor SQ-100X-SS (Apogee, USA). PAR beneath the canopy (PAR_b) at a height of 10 cm was measured using a line-type PAR sensor SQ-301X-SS (Apogee, USA) in each transplanting system in 2023. Solar radiation beneath the canopy (SR_b) at a height of 10 cm was measured using a line-type solarimeter PCM-200 (Prede, Japan) in each transplanting system in 2022. Data were sampled every second, averaged, and recorded every minute by a data logger CR-1000 (Campbell Scientific, USA). Wind speed (u) and rainfall (R) at a height of 2.0 m were measured using an all-in-one weather station ATMOS 41 (METER Group, USA) and recorded every minute by a data logger ZL6 (METER Group, USA). The general meteorological conditions (i.e., *SR*, T_a, RH, PAR_a, u, and R) were measured in the middle of the research plot, as illustrated in Figure 1a, and the PAR_b sensor was installed in each transplanting system. These sensors were installed on 7 DAT in 2022 and 8 DAT in 2023. For simplicity, the general meteorological data are displayed from 10 DAT to 110 DAT (the harvesting day). However, *SR* data before the installation day were obtained from *SR* data observed at the Matsuyama weather station [26], calibrated by the relationship between *SR* observed by the Matsuyama weather station and our sensor.

The light extinction coefficient of the leaf (k_l) in each transplanting system throughout the growing stage was analyzed using a modified equation for the mono-layer model of the canopy extinction coefficient introduced by Monsi and Saeki [27], as shown in Equations 4–7. The modification involved dividing the extinction parameters into the parameters for the leaf (k_l), stem (k_s), and panicle (k_p) because the panicle significantly contributes to shading the canopy, particularly after heading [28]. In 2022, k_l was calculated from solar radiation (Equation 4), and in 2023, k_l was calculated from PAR (Equation 5).

$$k_l(\mathrm{SR}) = \frac{-\ln\left(\frac{\mathrm{SR}_b}{\mathrm{SR}}\right) - k_s\,\mathrm{SAI} - k_p\,\mathrm{PAI}}{\mathrm{LAI}} \tag{4}$$

$$k_l(\mathrm{PAR}) = \frac{-\ln\left(\frac{\mathrm{PAR}_b}{\mathrm{PAR}_a}\right) - k_s\,\mathrm{SAI} - k_p\,\mathrm{PAI}}{\mathrm{LAI}} \tag{5}$$

$$\mathrm{SR}_b = \mathrm{SR}\exp\left(-(k_l\,\mathrm{LAI} + k_s\,\mathrm{SAI} + k_p\,\mathrm{PAI})\right) \tag{6}$$

$$\mathrm{SR}_{int} = \mathrm{SR} - \mathrm{SR}_b \tag{7}$$

where k_l(SR) and k_l(PAR) are the light extinction coefficients of solar radiation for leaves based on solar radiation and PAR, respectively. Then, k_s and k_p are the light extinction coefficients for leaves, stems, and panicles, respectively. LAI, SAI and PAI are leaf, stem and panicle area indices of the whole canopy, respectively. SR and SR_b (MJ m^{-2}) are the downward solar radiation above and beneath the canopy, respectively. PAR_a and PAR_b (µmol m^{-2} s^{-1}) are the PAR above and beneath the canopy, respectively. SR_{int} (MJ m^{-2}) is the calculated intercepted solar radiation by the canopy. SR in Equations 4, 6, and 7 were measured using CNR4 in both years. k_l in Equation 6 is k_l(SR) for the data in 2022 and k_l(PAR) for the calculation in 2023. The values for k_s were set at 0.10–0.14 and 0.07–0.10 for TL and JM, respectively. The values for k_p were set at 0.45–0.70 and 0.35–0.60 for TL and JM, respectively. Furthermore, k_s and k_p for JL were assumed to be the same as those in JM. The values of k_s and k_p were set based on a previous study [28]. Variations in k_s and k_p values throughout the growing stages followed the power curve functions. The values of k_s and k_p for PAR were assumed to be the same as the k_s and k_p values for SR.

Radiation use efficiency (RUE) has been widely used in crop growth analysis [29]. In this study, RUE is used to understand the effect of changes in intercepted solar radiation on the produced biomass in each transplanting system. The calculation of RUE is displayed in Equation 8.

$$\mathrm{RUE} = \frac{W_t}{\mathrm{SR}_{int}} \tag{8}$$

where RUE (g MJ^{-1}) is the radiation use efficiency of total above-ground biomass, W_t (g m^{-2}) is the total above-ground biomass, and SR_{int} (MJ m^{-2}) is the total solar radiation intercepted by the canopy, calculated using Equation 7.

Measurements of Normalized Difference Vegetation Index (NDVI)

The normalized difference vegetation index (NDVI) was measured using an NDVI camera Yubaflex (Bizworks, Japan) attached to an unmanned aerial vehicle (UAV) DJI Mavic Pro 2 (Shenzhen DJI Sciences and Technologies, China). NDVI values measured by the camera were calibrated with the NDVI measured by a spectral reflectance sensor (METER Group). The calibration formula was a combination of the calibration reported by a previous study [14] using the same device at the same research location to calibrate the NDVI of vegetation and the calibration of soil and water surfaces in 2023. NDVI was measured weekly from July 22 to September 30, 2023, under clear and stable sky conditions. Supervised classification was conducted to filter NDVI values of the plant body only, avoiding influence from other surfaces (i.e., soil and water surfaces). NDVI was calculated from the radiance of red light (reflected by the plant body) and the radiance of near-infrared light emitted by the plant body, as shown in Equation 9. The calibration formula is shown in Equation 10. Additionally, the irradiance of the red and near-infrared spectrum was measured by a spectral sensor S2-111-SS (Apogee, USA) at the same height as the CNR4.

$$\mathrm{NDVI} = \frac{L_{NIR} - L_{red}}{L_{NIR} + L_{red}} \quad (9)$$

$$\mathrm{NDVI}_{SRS} = -0.9742\ \mathrm{NDVI}_{camera}^{2} + 1.0837\ \mathrm{NDVI}_{camera} + 0.6296\ (R^2=0.9953) \quad (10)$$

where NDVI is the normalized difference vegetation index of the plant body only, L_{NIR} is the amount of near-infrared light reflected by the rice plant body, L_{red} is the amount of red light reflected by the plant body, NDVI_{SRS} is the NDVI measured by the spectral reflectance sensor (SRS), and NDVI_{camera} is the NDVI measured by the NDVI camera.

Results and Discussion

Meteorological Conditions

The timely variations of general meteorological variables are shown in Figure 2. The seasonal average of solar radiation above the canopy (SR) was slightly lower in 2023 than in 2022, with 198.3 W m^{-2} in 2023 and 206.0 W m^{-2} in 2022. Additionally, seasonal rainfall (R) was higher in the initial stage of 2023 compared to 2022 but lower during the maximum tiller-maturity stages in 2023 compared to 2022. The hourly average of air temperature (T_a) in 2023 was slightly higher than in 2022. Most importantly, the hourly average of T_a during the heading-maturity stages was 17.08–33.68 °C in 2022 and 16.21–34.77 °C in 2023. These T_a values were suitable for rice growth [30], but on some days, T_a exceeded 35.0 °C. Such conditions are expected to affect rice growth, potentially leading to a lower rice yield in 2023 than in 2022. A very high T_a might negatively impact rice yield, as reported by a previous study [31], which found that very high T_a (around 34 °C) could decrease grain weight.

Comparison of Plant Growth Parameters

The weekly variations in canopy height were similar between the transplanting systems, as shown in Figure 3a and 3b. The transplanting systems did not affect the canopy height of the Nikomaru rice cultivar. Consistent with this result, previous studies reported that double-row transplanting systems for Indica rice cultivars showed no significant difference in canopy height between TL and JL [32] and TL and JM [12]. In contrast to canopy height, the tiller number was affected by the space adjustment in JM and JL. JM and JL experienced higher competition for light than TL, resulting in a lower tiller number per hill. JL had the lowest tiller number per hill (Figure 3c and 3d), followed by JM and TL, due to the closer spacing between plants in JL and JM compared to TL. However, the denser plant density in JM and JL compared to TL resulted in a higher tiller number per unit area in both years, as shown in Figure 3e and 3f. These findings align with previous studies that reported increasing plant density through space adjustment reduced the tiller number per plant but increased the tiller number per unit area [33,34]. Comparing the tiller numbers in 2022 and 2023, the lower tiller number in 2023 was caused by higher T_a in the initial stage of 2023. The maxima of the hourly average T_a during the transplanting to the maximum tiller number stage were 33.78 °C in 2022 and 35.06 °C in 2023. Previous studies [30,35] reported that the number of tillers decreases due to high T_a, with the maximum T_a for the tillering stage reported as 33 °C [30]. Additionally, higher R and lower SR during the initial stage in 2023 exacerbated the impact on the tillering stage. These poor weather conditions during the initial growing stage to the maximum tiller stage in 2023 might have affected LAI, production, and yield, which will be discussed in the following results and discussion sections.

Weekly variations of LAI in each transplanting system in 2022 and 2023 are shown in Figure 3g and 3h. LAI increased throughout the growing stages, reached its maximum value around the heading stage, and decreased afterward. The double-row transplanting systems achieved higher LAI than the standard tile in both years. In 2022, JM obtained the highest LAI during the flag leaf extension–grain filling stages, followed by JL. In 2023, JM exhibited the same pattern, but the difference with JL was insignificant. Previous studies reported that denser planting density could increase LAI but would decline at a very high planting density [34]. In this study, both dense transplanting systems (JM and JL) achieved a higher LAI than the sparsest one (TL). The possible reason was that the higher population in JM and JL resulted in higher leaf biomass per unit area. Usually, in a very high planting density, biomass might decline. The following subsection will examine the biomass in each transplanting system.

Although LAI was lower in 2023 than in 2022, the stems were more leaned in 2023, resulting in lower leaf and panicle angles. This condition caused lower transmission of solar radiation at the ground or water surface in 2023 compared to 2022, as shown in Figure 4. Therefore, the meteorological properties, which will be discussed in the next subsection, cannot be compared between the years. However, these properties can be compared between the transplanting systems because the conditions in each transplanting system were similar (based on images of the rice canopy taken by drone). The weather conditions did not affect the canopy's erectness because the wind speed and rainfall were not high enough to bend the rice stems. Soil hardness is considered to be one of the reasons for the skewed stems in 2023 because mid-season drainage was not applied that year. One of the advantages of mid-season drainage is higher soil hardness, which allows roots to grip the soil firmly and the stems to stand upright [36], as observed in 2022.

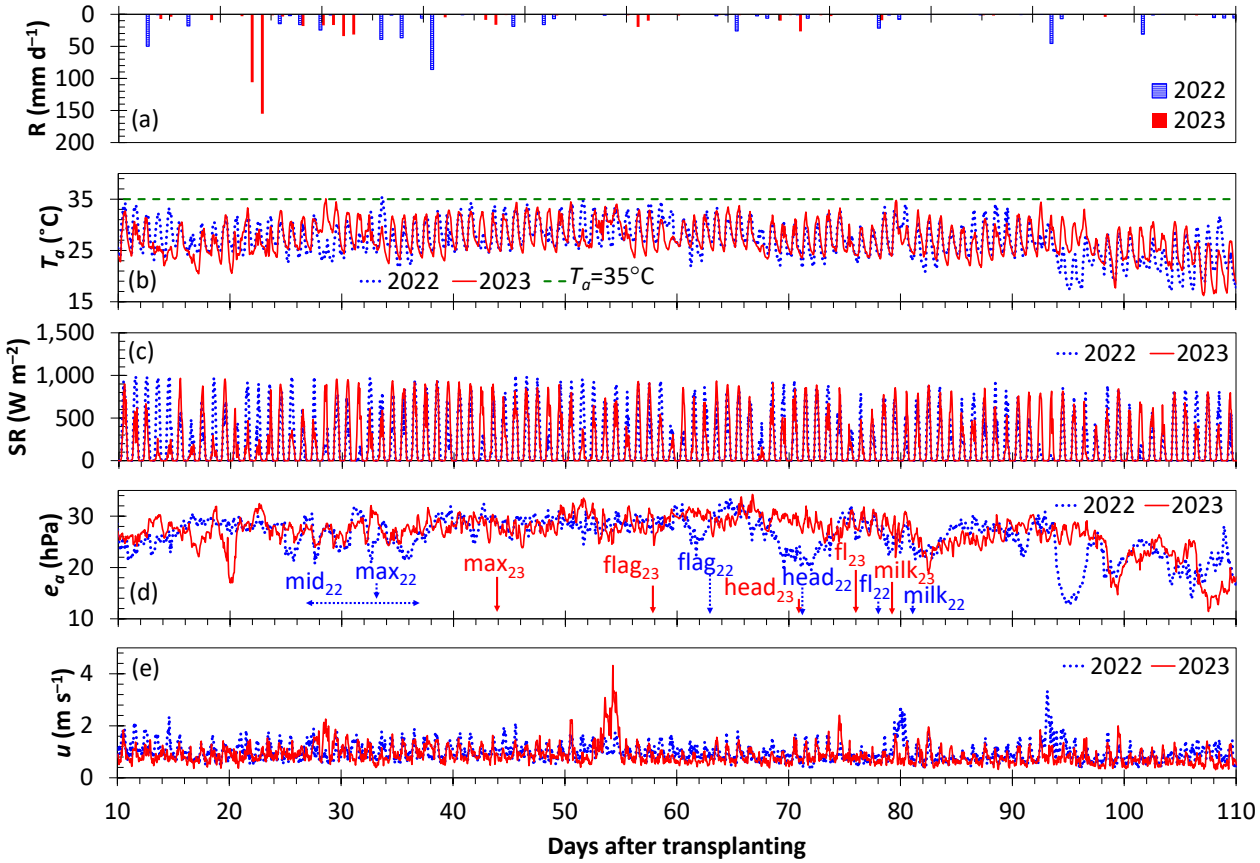

Figure 2. Variations of (a) daily precipitation (R), hourly average of (b) air temperature (T_a), (c) downward solar radiation (SR), (d) vapor pressure of air (e_a), and (e) wind speed (u) from 10 days after transplanting (DAT) to the harvesting day on 110 DAT in 2022 and 2023. The notes in Figure 2d indicate important phenological events, viz., mid-season drainage (mid), maximum tiller (max), flag leaf extension (flag), heading day (head), and 100% flowering (fl). The subscripted numbers (22 and 23) in these phenological events represent the year of the experiment (2022 and 2023, respectively).

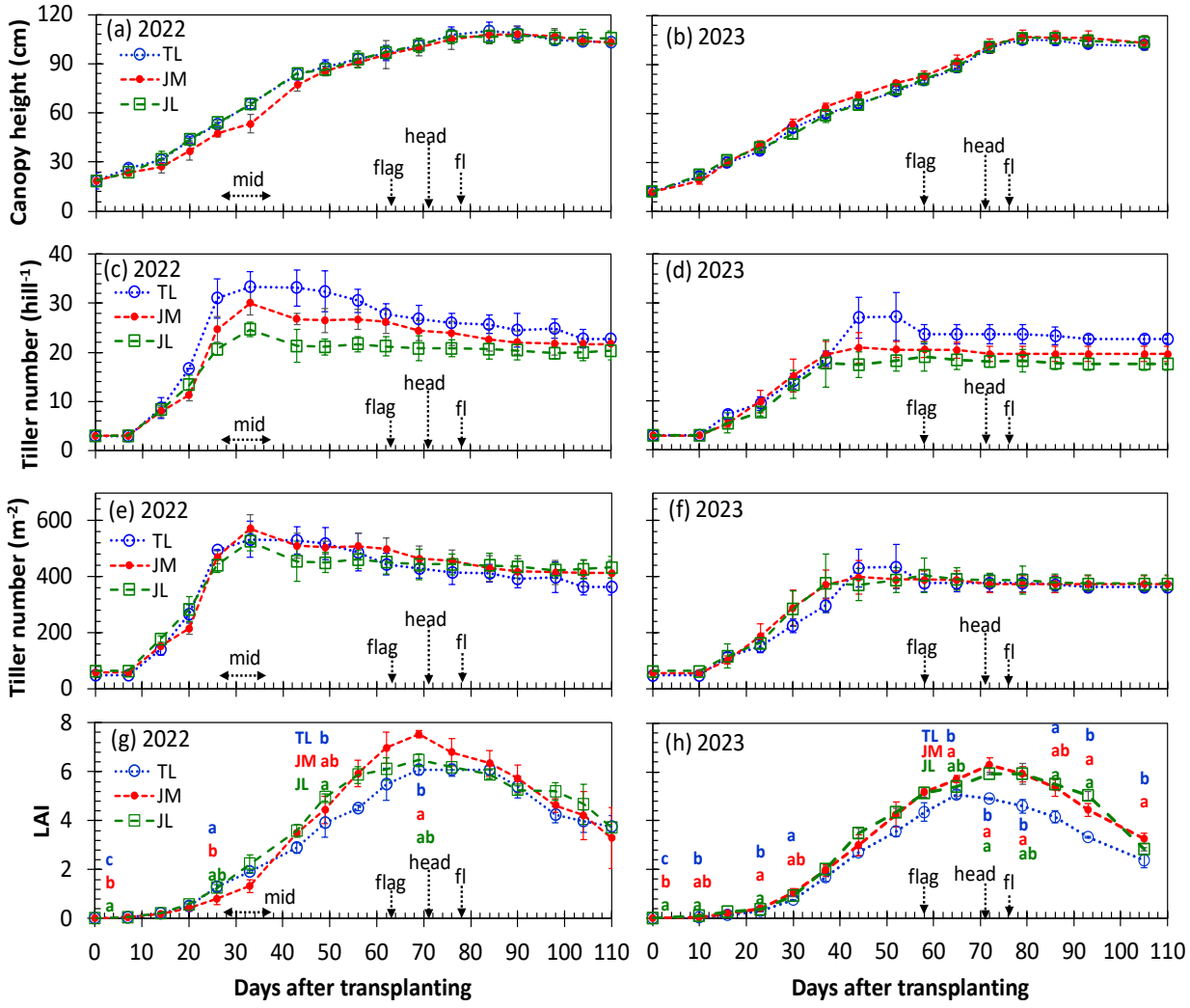

Figure 3. Weekly variations of (a–b) canopy height, (c–d) tiller number per hill, (e–f) tiller number per unit area, and (g–f) leaf area index of rice from the transplanting day to harvesting day in 2022 and 2023. The bars in the markers indicate the standard deviation. The notes of mid, flag, head, fl, and milk denote important phenological events, which are mid-season drainage, flag leaf extension, heading, flowering (100%), and milking (100%) stages, respectively. The letters above and below the markers indicate the significance of the data. The same letters indicate no significant difference (t-test with α=0.05, corrected by the Bonferroni test). The research data for 2022 is from Yuliawan et al. [22].

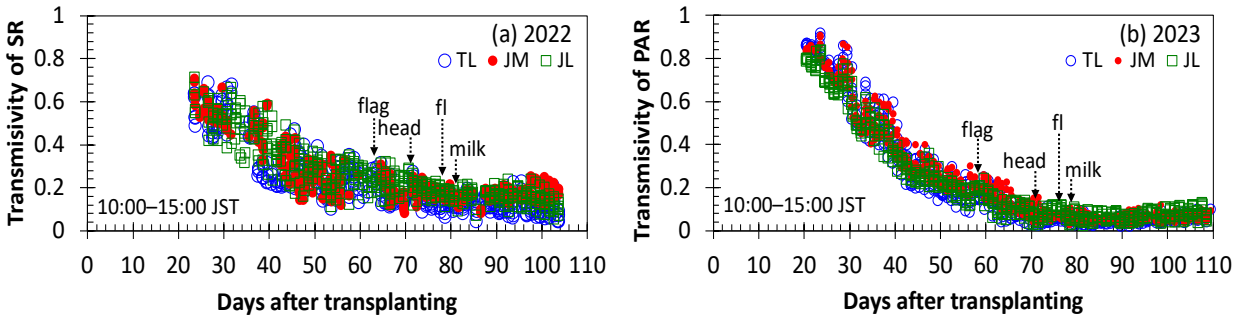

Figure 4. Hourly variations of transmissivity of (a) solar radiation in 2022 and (b) photosynthetically active radiation (PAR) in 2023 beneath the canopy. The notes of flag, head, fl, and milk denote the important phenological events, which are flag leaf extension, heading, flowering (100%), and milking (100%) stages, respectively.

Rice Production, Yield, and Its Components

The comparison of above-ground biomass in 2022 and 2023 is shown in Figure 5. JM and JL obtained higher above-ground biomass (W_t) per unit area, which was significantly different in 2022 but not significant in 2023. The W_t values were 17.44, 20.50, and 20.06 in 2022 and 15.10, 17.18, and 15.97 in 2023 for TL, JM, and JL, respectively. These results are comparable with the total above-ground biomass of other Japonica cultivars, such as Takanari and Akihikari, as reported by Katsura et al. [29]. This study observed that denser plants in JM and JL obtained lower above-ground biomass per hill (Figure 5b, 5e, and 5h) but higher above-ground biomass per unit area (Figure 5a, 5d, and 5g). When comparing the years, total above-ground biomass was higher in 2022 than in 2023 due to a higher T_a and lower SR in the initial stage in 2023 (Figure 2c). As explained in the previous sub-chapter, higher T_a and lower SR affected the period after transplanting to the maximum tiller number stage, resulting in a lower tiller number in 2023 than in 2022. Comparing biomass per hill, TL obtained the highest W_t, W_l, and W_s, followed by JM and JL (Figure 5b, 5e, and 5h). The biomass per tiller was insignificantly different among the transplanting systems. Adjusting the spacing in JM and JL could increase plant density, which could be both an advantage and a disadvantage. The disadvantage of denser plants in JM and JL was that these systems faced more competition for light, resulting in a lower above-ground biomass per hill (Figure 5b, 5e, and 5h). However, the denser plants in JM and JL increased above-ground biomass per unit area (Figure 5b, 5e, and 5h).

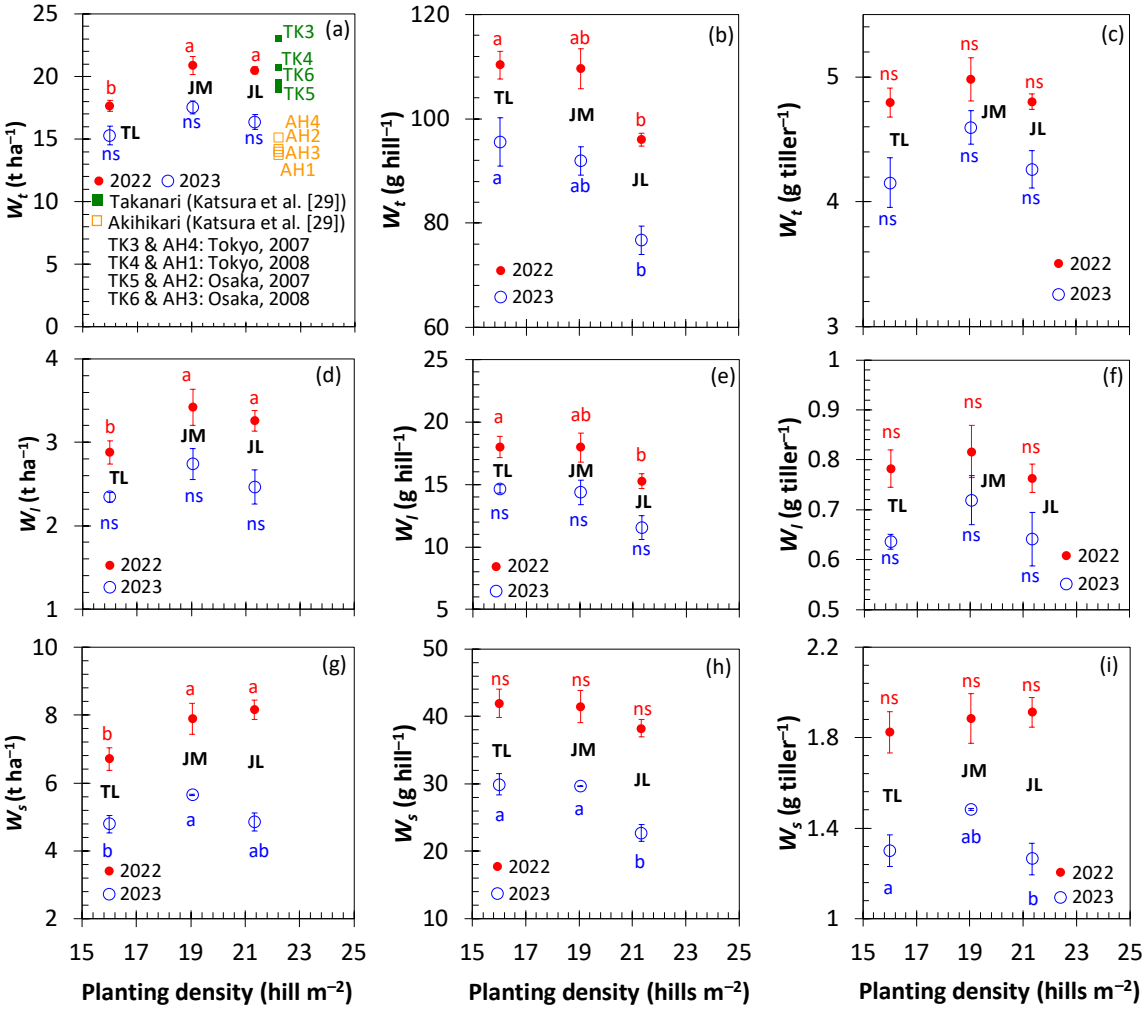

Figure 5. Comparison of total above-ground biomass (a) per unit area, (b) per hill, and (c) per tiller; dry weight of leaf (d) per unit area, (e) per hill, and (f) per tiller; and dry weight of stem (g) per unit area, (h) per hill, and (i) per tiller of the harvested samples in 2022 and 2023. The bars in the markers indicate the standard deviation. The letters above and below the markers indicate the significance of the data. The same letters are not significantly different (t-test with α=0.05, corrected by the Bonferroni test), and ns indicates not significant. The research data for 2022 is from Yuliawan et al. [22], and the total above-ground biomass of Takanari and Akihikari cultivars is from Katsura et al. [29].

The comparison of total grain number, weight of 1,000 grains, percentage of filled grain, and filled grain number per unit area of the harvested samples in 2022 and 2023 is shown in Figure 6. In line with the lower tiller number per hill in JM and JL due to higher competition in light, TL obtained the highest number of grains per hill, followed by JM and JL (Figure 6b). However, the denser plants in JM and JL increased the number of grains per unit area (Figure 6c). The percentage of filled grain was not significantly different among the transplanting systems (Figure 6e). However, JM had the highest filled grain per unit area, followed by JL and TL (Figure 6f). TL obtained the highest grain number per hill (Figure 6b) but the lowest percentage of filled grain per hill (Figure 6e). Some tillers in TL were young tillers, resulting in ineffective panicles for grain filling. As shown in Figure 3c and 3d, the highest reduction in tillers number was observed in TL, not only during the vegetative stage but also during the generative stage. The percentage of filled grain was also affected by the amount of absorbed solar radiation by the canopy, which will be discussed in the following subsection. Comparing the weight of 1,000 grains, the weight of 1,000 grains was not significantly different among the transplanting systems (Figure 6d).

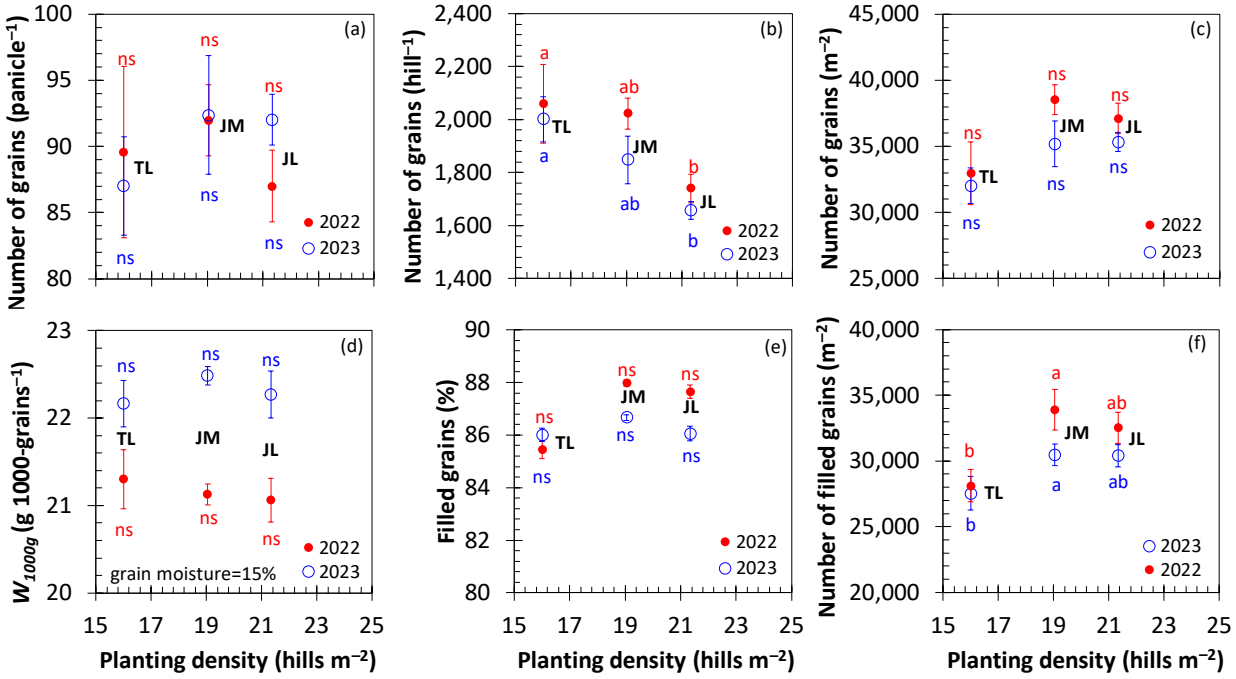

Figure 6. Comparison of the number of grains (a) per panicle, (b) per hill, and (c) per unit area; (d) weight of 1,000 grains ($W_{1,000g}$); (e) percentage of filled grains; and (f) number of filled grains per unit area of the harvested samples in 2022 and 2023. The bars in the markers indicate the standard deviation. The letters above and below the markers indicate the significance of the data. The same letters indicate no significant difference (t-test with α=0.05, corrected by the Bonferroni test), and ns indicates not significant. The research data for 2022 is from Yuliawan et al. [22].

In line with the higher number of filled grains, JM obtained the highest yield, followed by JL and TL (Figure 7a). Although higher competition in JM and JL caused a lower sink capacity per hill than in TL (Figure 7e), the higher sink capacity per unit area (Figure 7d) could increase the yield (Figure 7a). JM achieved the highest sink capacity per unit area, followed by JL and TL, as shown in Figure 7d. Denser plants in JM and JL resulted in lower tillers per hill, leading to a lower sink capacity per hill in TL (Figure 7e). However, JM and JL obtained higher sink capacities due to a higher population per unit area compared to TL (Figure 7d). A higher sink capacity per hill in TL compared to JM and JL is a disadvantage for TL. In a standard tile transplanting system, higher sink capacity often leads to a lower sink filling rate, as reported by previous research [37] on other Japonica cultivars. Additionally, the sink filling rate is influenced by the canopy's ability to intercept solar radiation, and TL may intercept less solar radiation due to lower LAI. However, JM and JL may also capture less solar radiation due to leaf shading in a dense canopy. The following subsection will investigate the intercepted solar radiation by the canopy.

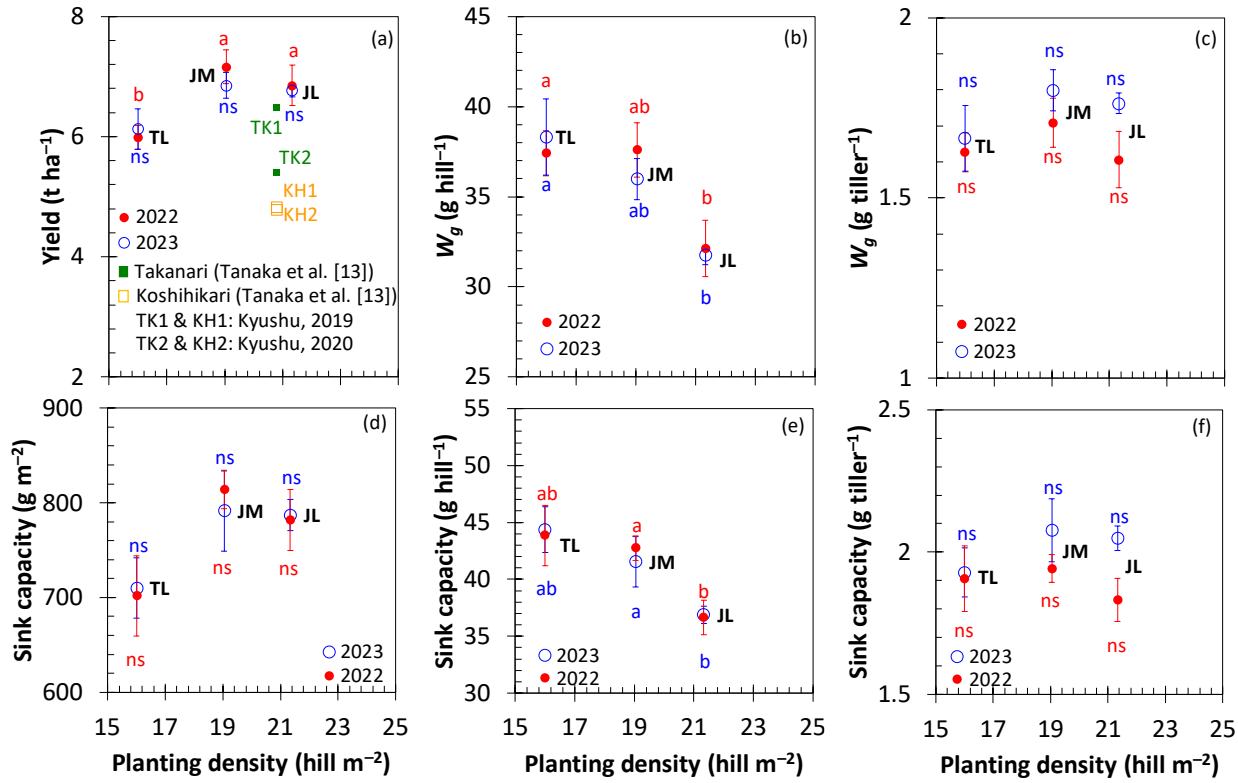

Figure 7. Comparison of (a) yield; weight of harvested grain (b) per hill, and (c) per tiller; sink capacity (d) per unit area, (e) per hill, and (f) per tiller of harvested sample in 2022 and 2023. The bars in the markers indicate the standard deviation. The letters above and below the markers indicate the significance of the data. The same letters indicate no significant difference (t-test with α=0.05, corrected by the Bonferroni test), and ns indicates not significant. The research data for 2022 is from Yuliawan et al. [22], and the yield of Takanari and Koshihikari cultivars is from Tanaka et al. [13].

Interception of Solar Radiation by The Canopy

As explained in the previous sections, JM obtained the highest LAI, followed by JL (Figure 3g and 3h). However, the larger spacing might be a disadvantage for JM and JL in terms of solar radiation interception. Figure 8 shows that during the initial–flowering stages, the values of canopy extinction coefficient for solar radiation, k_l (SR), and canopy extinction coefficient for PAR, k_l (PAR), were nearly constant due to leaf erectness. However, during the flowering–maturity stages, the values increased following the power curve due to lower leaf angle caused by panicle appearance and senescence. These results align with previous research [38] on the Koshihikari cultivar in the Kyushu region of Japan (planting density = 20.83 hills m^{-2}), which showed k_l values around 0.3–1.0, following the power curve. A high k_l value corresponds to low transmitted solar radiation to the ground surface, and vice versa.

As shown in Figure 8, TL obtained the highest k_l (SR) and k_l (PAR), while JM and JL were comparable. In 2023, about ten days before harvesting, the k_l(PAR) values in TL were close to 1.0 because the closer spacing between the plants in TL than in JM and JL caused greater shading by the upper canopy layer to the lower canopy layer, even though TL had the lowest LAI. Additionally, soil hardness was lower in 2023 than in 2022, so the plants could not stand as well as in 2022. On the other hand, despite the larger LAI in JM and JL than in TL, the wider spacing in both caused greater penetration of solar radiation to the lower layer, resulting in lower k_l (SR) and k_l (PAR). However, the average intercepted solar radiation was not significantly different between the transplanting systems in 2023. In 2022, JM obtained the highest intercepted SR during the flag leaf extension to milking stages (Figure 8b), which are the most important growing stages for grain filling.

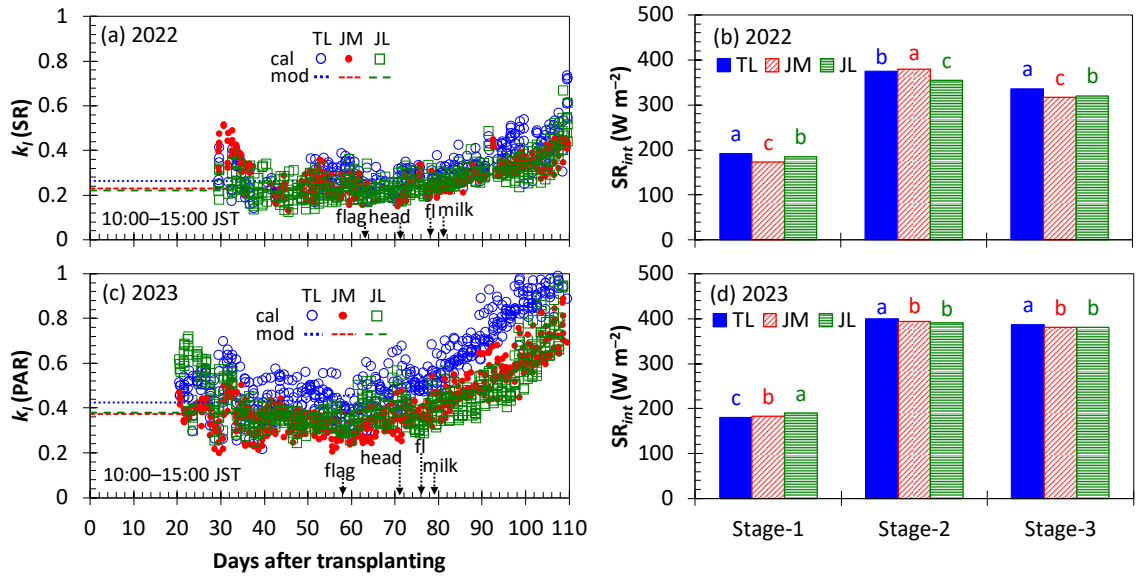

Figure 8. Hourly variations of (a) k_l (SR) in 2022 and (c) k_l (PAR) in 2023, and the average intercepted solar radiation in (b) 2022 and (d) 2023 in each transplanting system. k_l (SR) and k_l (PAR) are the extinction coefficients for solar radiation and photosynthetically active radiation, respectively. The notes of flag, head, fl, and milk denote important phenological events, which are flag leaf extension, heading, flowering (100%), and milking (100%) stages, respectively. Stage-1 is from transplanting to before the flag extension stage, Stage-2 is from flag extension to milking (100%) stages, and Stage-3 is from after milking (100%) stage to harvest. The modeled k_l is fitted to the power curve functions of the calculated k_l.

The comparisons of RUE and the relationship between sink capacity and sink filling rate are shown in Figure 9. JM obtained the highest RUE, followed by JL and TL in both years (Figure 9a). The double-row transplanting systems used in this study could produce biomass more efficiently due to the denser planting compared to the standard tile. Although TL obtained higher k_l (SR) and k_l (PAR) than JM and JL (Figure 8a and 8c), the intercepted solar radiation by the canopy was not significantly different from JM and JL in 2023, and was lower than JM in 2022, particularly during the flag leaf extension to milking stages. Additionally, TL obtained the highest sink capacity per hill due to the highest tiller number. Hence, the utilization of absorbed solar radiation for grain filling was ineffective in TL, as indicated by the lower sink filling rate in TL compared to JM and JL, as shown in Figure 9b and will be discussed in the following subsection. A higher sink capacity in JM and JL per unit area resulted in a higher yield compared to TL.

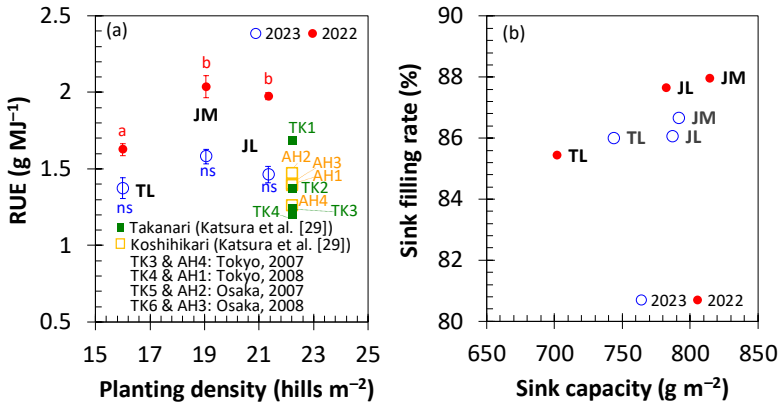

Figure 9. Comparisons of (a) radiation use efficiency (RUE) and the relationship between sink capacity and sink filling rate (b) per unit area and (c) per hill in 2022 and 2023. The bars in the markers indicate the standard deviation, and ns indicates not significant. The data on sink capacity and sink filling rate in 2022 are from Yuliawan et al. [22], and the data on the RUE of Takanari and Akihikari cultivars are from Katsura et al. [29].

Normalized Difference Vegetation Index

JM obtained the highest normalized difference vegetation index (NDVI), followed by JL and TL (Figure 10a). Although the differences among the transplanting systems are not significant, JM achieved a higher NDVI throughout the entire growing stage, with JL obtaining similar NDVI values after the milking stage. These results correlate to the LAI variations shown in Figure 3g and 3h, where JM obtained the highest LAI, followed by JL and TL.

Besides detecting vegetation density, NDVI can describe canopy health conditions, where higher NDVI indicates a healthier canopy capable of utilizing absorbed solar radiation optimally [16]. As shown in Figure 10b, the reflected red spectrum was lower in JM and JL, suggesting that the canopies of JM and JL absorbed more visible light for photosynthetic activity. Because yield was strongly correlated with biomass during the heading–grain filling stage (e.g., [39]), the highest NDVI obtained by JM, particularly during the flag leaf extension to milking stage, has the potential to increase the utilization of absorbed solar radiation for grain filling. After analyzing correlations between NDVI and sink filling rate and yield, this study found that the average NDVI during the flag leaf extension to milking stages had the highest coefficient of determination. As shown in Figure 10d and 10e, the average NDVI during the flag leaf extension to milking stages was strongly correlated with the sink filling rate and yield. The lower NDVI and lower reflected red spectrum in TL compared to JM and JL could be due to the horizontal distribution of leaves in the upper layer TL, which allows these leaves to intercept solar radiation in the upper layer but shade the middle layer, leading to a higher senescence rate. This issue will be discussed in detail using the multi-layer model approach in an upcoming study.

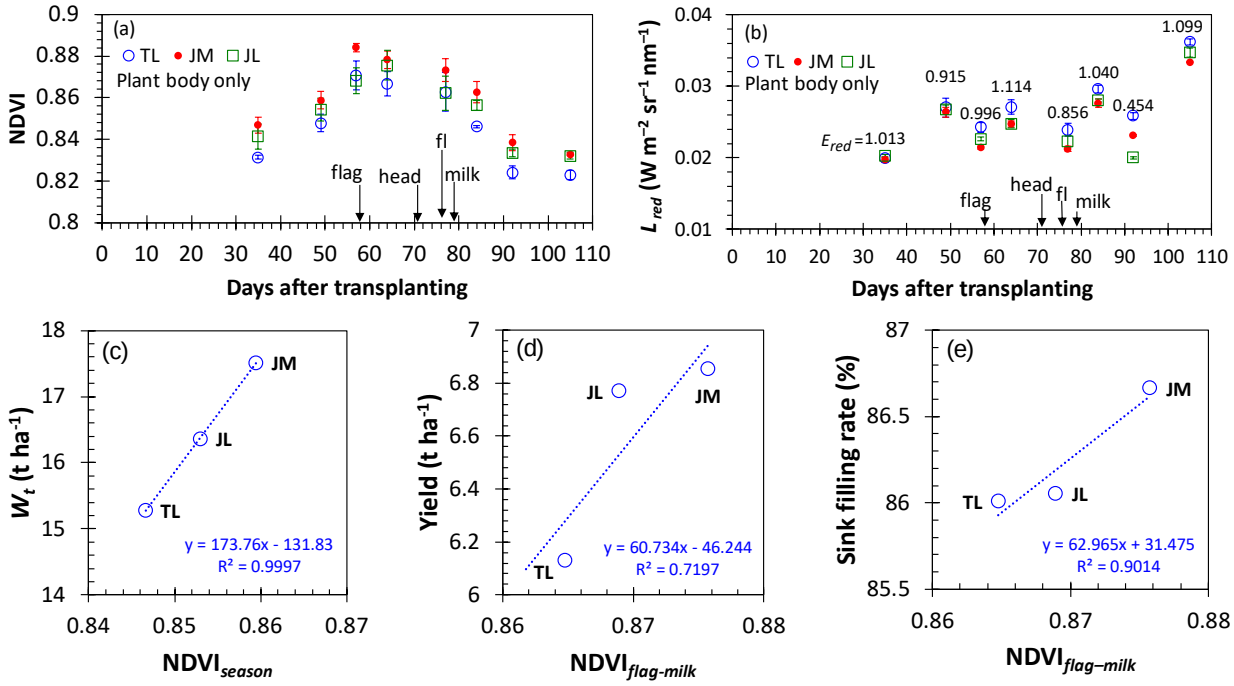

Figure 10. Weekly variations of (a) normalized difference vegetation index (NDVI), (b) radiance of red spectrum (L_{red}) reflected by the canopy, and the relationships between (c) the average of NDVI throughout the season and total above-ground biomass, (d) the average of NDVI during the grain filling stage (flag leaf extension–milking, NDVI$_{flag–milk}$), and (e) NDVI$_{flag–milk}$ and sink filling rate. The bars in the markers indicate the standard deviation. The notes of flag, head, fl, and milk denote important phenological events, which are flag leaf extension, heading, flowering (100%), and milking (100%) stages, respectively. The numbers above the markers in Figure 10b indicate the irradiance of the red spectrum (E_{red}).

The schematic diagram of the effect of the double-row transplanting system on rice yield is shown in Figure 11. Besides increased planting density, space adjustment in JM and JL can improve the absorption of solar radiation. Typically, a dense canopy can reduce solar radiation due to leaf shading. However, the larger space between the double rows and higher LAI in JM and JL can increase the absorption of solar radiation, similar

to TL. Furthermore, higher NDVI in JM and JL compared to TL might enhance the utilization of intercepted solar radiation for grain filling, resulting in a higher sink filling rate. Space adjustment in JM and JL could achieve the border effect and increase yield. Previous research has shown that the border effect can increase rice yield by increasing the sink capacity, which is the grain number per unit area [40] and the number of filled grains per unit area [20]. Comparing JM and JL, JM achieved a more optimal border effect due to the wider space between the double rows and the columns. This study suggests that JM is the best transplanting system for increasing rice yield and also recommends JL as an alternative option. Besides obtaining a higher yield than the standard tile, the wider space in JM and JL makes field management easier than in TL. The government should continue to promote JL as a selected transplanting system in the national agricultural program and consider including JM in that national program promotion. However, those double-row transplanting systems should be investigated across various rice cultivars to understand the differences in growth, yield, and meteorological properties under different types of rice canopy.

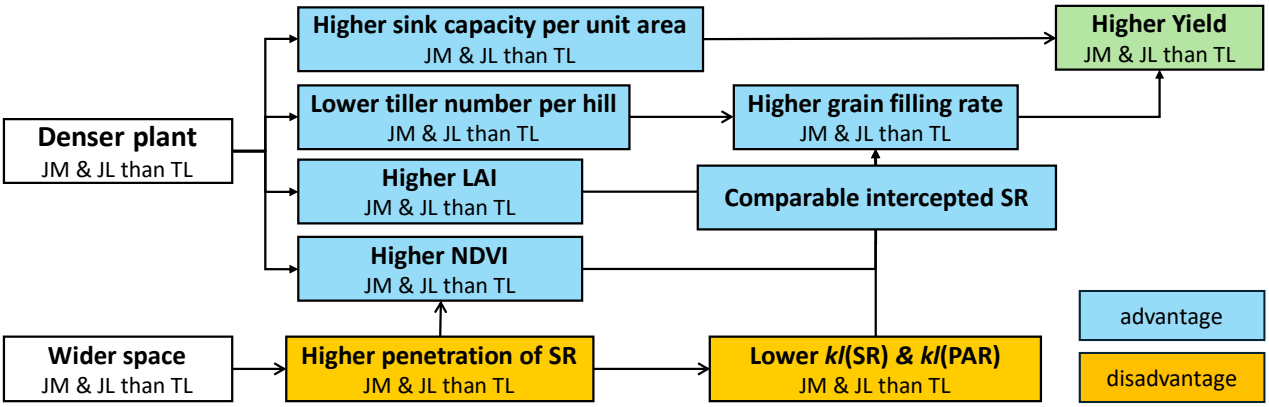

Figure 11. The schematic diagram of the effect of the double-row transplanting system on rice yield.

Advanced analysis is needed to understand the impact of the border effect on JM and JL. In an upcoming study, a multi-layer model will be used to investigate how the leaves contribute to intercepting solar radiation in different canopy layers (for example, every 10 cm of canopy height). This multi-layer model will also reveal the vertical profiles of parameters related to the contribution of the leaves in capturing solar radiation, which will be correlated with the NDVI values and photosynthetic rates of the rice canopy. This approach will provide a detailed understanding of the environmental changes within the canopy of JM and JL.

Conclusions

This study revealed differences in growth, yield, and meteorological properties between the double-row transplanting systems *Jajar Legowo* (JL) and *Jejer Manten* (JM), as well as the standard tile transplanting system (TL). Besides testing these transplanting systems on a Japonica rice cultivar (Nikomaru) to increase rice yield, the findings aimed to address the lack of scientific evidence on the advantages of JL and JM. JM obtained the highest yield, followed by JL and TL. The synergistic effect of higher sink capacity and sink filling rate in JM and JL led to a higher yield than in TL. Although higher plant competition for light in JM and JL caused a lower tiller number and above-ground biomass per hill than in TL, JM and JL achieved higher tiller numbers and above-ground biomass per unit area due to denser plants. The denser plants increased the sink capacity per unit area in JM and JL compared to TL. Additionally, the denser canopy in JM and JL compared to TL increased the intercepted solar radiation by the whole canopy (SR_{int}) despite the wider space between the double rows. Although SR_{int} was not significantly different among the systems, higher NDVI in JM and JL compared to TL was strongly correlated with a higher sink filling rate due to the healthier canopy absorbing more solar radiation. The synergistic effect of higher sink capacity and sink filling rate led to higher yields in JM and JL compared to TL. This study suggests that JM is the best transplanting system for increasing rice yield.

Author Contributions

TY: Conceptualization, Methodology, Investigation, Formal Analysis, Visualization, Writing - original draft; **NI**: Conceptualization, Methodology, Investigation; **AU**: Methodology, Investigation; **FI**: Methodology, Investigation, and **HO**: Conceptualization, Resources, Supervision, Validation, Writing - Review & Editing.

Conflicts of interest

There are no conflicts to declare.

Acknowledgments

We sincerely thank Prof. Takuya Araki from the Graduate School of Agriculture, Ehime University, for sharing resources for the field experiment. We would like to thank Dr. Yuto Hatakeyama, Mr. Kominami Tsukasa, Ms. Mirika Yamanaka, and their colleagues from The Laboratory of Crop Science, Ehime University, for their advice. This research was partially supported by the JSPS KAKENHI (grant number: J21K05851) and MEXT. The first author would like to thank the MEXT scholarship for supporting his research activities in Japan.

References

1. USDA (United States Department of Agriculture). Production, Supply and Distribution Online Database Available online: https://apps.fas.usda.gov/psdonline (accessed on 10 December 2023).
2. IPCC (Intergovernmental Panel on Climate Change). *Climate Change 2022 – Impacts, Adaptation and Vulnerability: Working Group II Contribution to the Sixth Assessment Report of the Intergovernmental Panel on Climate Change*; Cambridge University Press: Cambridge, UK, 2023;
3. Peng, S.; Huang, J.; Sheehy, J.E.; Laza, R.C.; Visperas, R.M.; Zhong, X.; Centeno, G.S.; Khush, G.S.; Cassman, K.G. Rice Yields Decline with Higher Night Temperature from Global Warming. *Proceedings of the National Academy of Sciences* **2004**, *101*, 9971–9975, doi:10.1073/pnas.0403720101.
4. Masutomi, Y.; Takimoto, T.; Shimamura, M.; Manabe, T.; Arakawa, M.; Shibota, N.; Ooto, A.; Azuma, S.; Imai, Y.; Tamura, M. Rice Grain Quality Degradation and Economic Loss Due to Global Warming in Japan. *Environ Res Commun* **2019**, *1*, 121003, doi:10.1088/2515-7620/ab52e7.
5. Rawung, J.B.M.; Indrasti, R.; Sudolar, N.R. The Impact of Technological Innovation of Jajar Legowo 2:1 Planting System on Rice Business Income. *IOP Conference Series: Earth and Environmental Science* **2021**, *807*, 032052, doi:10.1088/1755-1315/807/3/032052.
6. Toyibah, E.S.; Sujarwo; Nugroho, C.P. Jajar Legowo Planting System as The Strategy on Climate Change Adaptation (Case Study in Srigading Village Lawang District, Malang). *Agricultural Socio-Economic Journal* **2016**, *16*, 25–30.
7. DEPTAN (Departemen Pertanian). *Minapadi Azolla Dengan Tanam Jajar Legowo (Teknologi Yang Digunakan Pada Penelitian Adaptif Pengembangan Varietas Padi Unggul Lokal Di Cianjur)*; DEPTAN: Lembang, ID, 1995;
8. Sarlan, A.; Made, J.M.; Nurwulan, A.; Indra, G.; Priatna, S.; Agus, G. *Sistem Tanam LEGOWO*; Suharna, Ed.; BB Padi: Sukamandi, ID, 2013;
9. Asnawi, R.; Arief, R.W.; Slameto, S.; Tambunan, R.D.; Martias, M.; Mejaya, M.J.; Fitriani, F. Increasing Rice (*Oryza sativa* L.) Productivity and Farmer's Income through the Implementation of Modified Double Rows Planting System. *Annu. Res. Rev. Biol.* **2021**, *36*, 42–52, doi:10.9734/arrb/2021/v36i830409.
10. Usman, M.; Anam, C.; Qibtiyah, M. Kajian Macam Pola Tanam Jajar Legowo Dan Kombinasi Pupuk Terhadap Pertumbuhan Dan Produksi Tanaman Padi (*Oryza sativa* L.). *AGRORADIX : Jurnal Ilmu Pertanian* **2019**, *2*, 59–71, doi:10.52166/agroteknologi.v2i2.1591.
11. Maisura, M.; Jamidi, J.; Husna, A. Respon Pertumbuhan Dan Hasil Tanaman Padi (*Oryza sativa* L.) Varietas IPB 3S Pada Beberapa Sistem Jajar Legowo. *Jurnal Agrium* **2020**, *17*, 33–44, doi:10.29103/agrium.v17i1.2353.

12. Asnawi, R.; Arief, R.W. Kajian Cara Tanam Jejer Manten Dan Pupuk Hayati Pada Usahatani Padi Sawah Di Kabupaten Pesawaran Provinsi Lampung. *Jurnal Pengkajian dan Pengembangan Teknologi Pertanian* **2016**, *19*, 93–102, doi:10.21082/jpptp.v19n2.2016.p93-102.
13. Tanaka, R.; Hakata, M.; Nakano, H. Grain Yield Response to Cultivar and Harvest Time of the First Crop in Rice Ratooning in Southwestern Japan. *Crop. Sci.* **2022**, *62*, 455–465, doi:10.1002/csc2.20645.
14. Irsyad, F.; Oue, H.; Mon, M.M. Monitoring Responses of NDVI and Canopy Temperature in a Rice Field to Soil Water and Meteorological Conditions. *IOP Conf. Ser. Earth. Environ. Sci.* **2022**, *1059*, 012037, doi:10.1088/1755-1315/1059/1/012037.
15. Kriegler, F.J.; Malila, W.A.; Nalepka, R.F.; Richardson, W. Preprocessing Transformations and Their Effects on Multispectral Recognition. In Proceedings of the 6th International Symposium on Remote Sensing of Environment, University of Michigan, Ann Arbor, Michigan, 1969, pp. 97-131.
16. Anamaria, R.; Tudor, U. Multispectral Satellite Imagery and Airborne Laser Scanning Techniques for the Detection of Archaeological Vegetation Marks. In *Landscape Archaeology on The Northern Frontier of The Roman Empire at Porolissum - an Interdisciplinary Research Project*; Coriolan, H., Vlad-Andrei, L., Eds.; Mega Publishing House: Cluj-Napoca, 2016; pp. 141–152, ISBN 978-606-543-787-6.
17. Gallo, K.P.; Daughtry, C.S.T.; Bauer, M.E. Spectral Estimation of Absorbed Photosynthetically Active Radiation in Corn Canopies. *Remote Sens. Environ.* **1985**, *17*, 221–232, doi:10.1016/0034-4257(85)90096-3.
18. Susilastuti, D.; Aditiameri, A.; Buchori, U. The Effect of Jajar Legowo Planting System on Ciherang Paddy Varieties. *AGRITROPICA: Journal of Agricultural Sciences* **2018**, *1*, 1–8.
19. Sato, K.; Takahashi, K. An Analysis of the Border Effect in the Rice Paddy Fields. *Japanese Journal of Crop Science* **1983**, *52*, 168–176, doi:10.1626/jcs.52.168.
20. Mak, M. Estimation of Border Effect on Yield of Rice and Nutrient Uptake. *International Journal of Agricultural Science and Food Technology* **2021**, 255–259, doi:10.17352/2455-815x.000116.
21. Wang, K.; Zhou, H.; Wang, B.; Jian, Z.; Wang, F.; Huang, J.; Nie, L.; Cui, K.; Peng, S. Quantification of Border Effect on Grain Yield Measurement of Hybrid Rice. *Field Crops Res.* **2013**, *141*, 47–54, doi:10.1016/j.fcr.2012.11.012.
22. Yuliawan, T.; Oue, H.; Ichwan, N.; Ukpoju, A. Comparison of Plant Growth and Yield of Rice under Double-Row and Tile Transplanting Systems. *IOP Conf. Ser. Earth Environ. Sci.* **2023**, *1182*, 12039, doi:10.1088/1755-1315/1182/1/012039.
23. Fukazawa, M.; Shirakawa, N. Effects of Inabenfide [4'-Chloro-2'-(α-Hydroxybenzyl)-Isonicotinanilide] on Growth, Lodging, and Yield Components of Rice. *Plant Prod. Sci.* **2001**, *4*, 118–125, doi:10.1626/pps.4.118.
24. Okamura, M.; Hosoi, J.; Nagata, K.; Koba, K.; Sugiura, D.; Arai-Sanoh, Y.; Kobayashi, N.; Kondo, M. Cross-Locational Experiments to Reveal Yield Potential and Yield-Determining Factors of the Rice Cultivar' Hokuriku 193' and Climatic Factors to Achieve High Brown Rice Yield over 1.2kg m-2 at Nagano in Central Inland of Japan. *Plant Prod. Sci.* **2022**, *25*, 131–147, doi:10.1080/1343943X.2021.1981140.
25. Yoshinaga, S.; Heinai, H.; Ohsumi, A.; Furuhata, M.; Ishimaru, T. Characteristics of Growth and Quality, and Factors Contributing to High Yield in Newly Developed Rice Variety 'Akidawara.' *Plant Prod. Sci.* **2018**, *21*, 186–192, doi:10.1080/1343943X.2018.1463165.
26. JMA (Japan Meteorological Agency). 過去の気象データ・ダウンロード (Download Historical Data). Available online: https://www.data.jma.go.jp/risk/obsdl/index.php (accessed on 11 February 2023).
27. Monsi, M.; Saeki, T. On the Factor Light in Plant Communities and Its Importance for Matter Production. *Ann. Bot.* **2005**, *95*, 549–567, doi:10.1093/aob/mci052.
28. Oue, H. Evapotranspiration, Photosynthesis and Water Use Efficiency in a Paddy Field (II) — Prediction of Energy Balance and Water Use Efficiency by Numerical Simulations Based on a Multilayer Model. *Journal Japan Society Hydrology and Water Resources* **2003**, *16*, 389–407, doi:10.3178/jjshwr.16.389.
29. Katsura, K.; Okami, M.; Mizunuma, H.; Kato, Y. Radiation Use Efficiency, N Accumulation and Biomass Production of High-Yielding Rice in Aerobic Culture. *Field Crops Res.* **2010**, *117*, 81–89, doi:10.1016/j.fcr.2010.02.006.
30. Yoshida, S. *Fundamentals of Rice Crop Science*; International Rice Research Institute: Los Banos, 1981;

31. Morita, S.; Shiratsuchi, H.; Takanishi, J.; Fujita, K. Effect of High Temperature on Ripening in Rice Plants: Comparison of the Effects of High Night Temperatures and High Day Temperatures (Crop Physiology and Cell Biology). *Japanese Journal of Crop Science* **2002**, *71*, 102–109, doi:10.1626/jcs.71.102.
32. Susilastuti, D.; Aditiameri, A.; Buchori, U. The Effect of Jajar Legowo Planting System on Ciherang Paddy Varieties. *AGRITROPICA* **2018**, *1*, 1–8, doi:10.31186/j.agritropica.1.1.1-8.
33. Clerget, B.; Bueno, C.; Domingo, A.J.; Layaoen, H.L.; Vial, L. Leaf Emergence, Tillering, Plant Growth, and Yield in Response to Plant Density in a High-Yielding Aerobic Rice Crop. *Field Crops Res.* **2016**, *199*, 52–64, doi:10.1016/j.fcr.2016.09.018.
34. Hu, Q.; Jiang, W.; Qiu, S.; Xing, Z.; Hu, Y.; Guo, B.; Liu, G.; Gao, H.; Zhang, H.; Wei, H. Effect of Wide-Narrow Row Arrangement in Mechanical Pot-Seedling Transplanting and Plant Density on Yield Formation and Grain Quality of Japonica Rice. *J. Integr. Agric.* **2020**, *19*, 1197–1214, doi:10.1016/S2095-3119(19)62800-5.
35. Xu, J.; Henry, A.; Sreenivasulu, N. Rice Yield Formation under High Day and Night Temperatures—A Prerequisite to Ensure Future Food Security. *Plant Cell Environ.* **2020**, *43*, 1595–1608, doi:10.1111/pce.13748.
36. Nishimura, S.; Kimiwada, K.; Yagioka, A.; Hayashi, S.; Oka, N. Effect of Intermittent Drainage in Reduction of Methane Emission from Paddy Soils in Hokkaido, Northern Japan. *Soil Sci. Plant Nutr.* **2020**, *66*, 360–368, doi:10.1080/00380768.2019.1706191.
37. Yoshinaga, S.; Heinai, H.; Ohsumi, A.; Furuhata, M.; Ishimaru, T. Characteristics of Growth and Quality, and Factors Contributing to High Yield in Newly Developed Rice Variety 'Akidawara.' *Plant Prod. Sci.* **2018**, *21*, 186–192, doi:10.1080/1343943X.2018.1463165.
38. Maruyama, A.; Kuwagata, T.; Ohba, K.; Maki, T. Dependence of Solar Radiation Transport in Rice Canopies on Developmental Stage. *JARQ* **2007**, *41*, 39–45, doi:10.6090/jarq.41.39.
39. Hatfield, J.L. Remote Sensing Estimators of Potential and Actual Crop Yield. *Remote Sens. Environ.* **1983**, *13*, 301–311, doi:10.1016/0034-4257(83)90032-9.
40. Zheng, C.; Wang, Y.C.; Xu, W.B.; Yang, D.S.; Yang, G.D.; Yang, C.; Huang, J.L.; Peng, S.B. Border Effects of the Main and Ratoon Crops in the Rice Ratooning System. *J. Integr. Agric.* **2023**, *22*, 80–91, doi:10.1016/j.jia.2022.08.048.